Physiologia Plantarum
An International Journal for Plant Biology

Physiologia Plantarum 152: 316–330. 2014 ISSN 0031-9317

Combined effects of different CO_2 levels and N sources on the diazotrophic cyanobacterium *Trichodesmium*

Meri Eichner[a,*], Sven A. Kranz[b] and Björn Rost[a]

[a]Marine Biogeosciences, Alfred-Wegener-Institut Helmholtz-Zentrum für Polar- und Meeresforschung, Bremerhaven 27570, Germany
[b]Department of Geosciences, Princeton University, Princeton, NJ, 08544, USA

Correspondence
*Corresponding author,
e-mail: meri.eichner@awi.de

Received 11 November 2013;
revised 17 January 2014

doi:10.1111/ppl.12172

To predict effects of climate change and possible feedbacks, it is crucial to understand the mechanisms behind CO_2 responses of biogeochemically relevant phytoplankton species. Previous experiments on the abundant N_2 fixers *Trichodesmium* demonstrated strong CO_2 responses, which were attributed to an energy reallocation between its carbon (C) and nitrogen (N) acquisition. Pursuing this hypothesis, we manipulated the cellular energy budget by growing *Trichodesmium erythraeum* IMS101 under different CO_2 partial pressure (pCO_2) levels (180, 380, 980 and 1400 µatm) and N sources (N_2 and NO_3^-). Subsequently, biomass production and the main energy-generating processes (photosynthesis and respiration) and energy-consuming processes (N_2 fixation and C acquisition) were measured. While oxygen fluxes and chlorophyll fluorescence indicated that energy generation and its diurnal cycle was neither affected by pCO_2 nor N source, cells differed in production rates and composition. Elevated pCO_2 increased N_2 fixation and organic C and N contents. The degree of stimulation was higher for nitrogenase activity than for cell contents, indicating a pCO_2 effect on the transfer efficiency from N_2 to biomass. pCO_2-dependent changes in the diurnal cycle of N_2 fixation correlated well with C affinities, confirming the interactions between N and C acquisition. Regarding effects of the N source, production rates were enhanced in NO_3^- grown cells, which we attribute to the higher N retention and lower ATP demand compared with N_2 fixation. pCO_2 effects on C affinity were less pronounced in NO_3^- users than N_2 fixers. Our study illustrates the necessity to understand energy budgets and fluxes under different environmental conditions for explaining indirect effects of rising pCO_2.

Introduction

The release of anthropogenic carbon (C) has caused atmospheric CO_2 partial pressure (pCO_2) to increase from 280 to 390 µatm since pre-industrial times and pCO_2 levels are expected to rise further to 750 µatm or even beyond 1000 µatm by the end of this century (IPCC 2007, Raupach et al. 2007). As CO_2 is taken up by the ocean, seawater CO_2 concentrations increase and pH levels decrease, a phenomenon termed ocean acidification (Caldeira and Wickett 2003). These changes in carbonate chemistry are expected to have diverse effects

Abbreviations – ARA, acetylene reduction assay; CA, carbonic anhydrase; CCM, carbon concentrating mechanism; chl *a*, chlorophyll *a*; C_i, inorganic carbon; DIC, dissolved inorganic carbon; Fv/Fm, PSII photochemical quantum yield measured in dark-adapted state; Fv′/Fm′, PSII photochemical quantum yield measured in light-adapted state; HEPES, 4-(2-hydroxylethyl)-1-piperazine-ethanesulfonic acid; HSD, honest significant difference; $K_{1/2}$, half-saturation concentration; pCO_2, CO_2 partial pressure; POC, particulate organic carbon; PON, particulate organic nitrogen; PQ, plastoquinone; RubisCO, ribulose-1,5-bisphosphate carboxylase/oxygenase; TA, total alkalinity; V_{max}, maximum rate; σ, PSII functional absorption cross section; τ, Q_A re-oxidation time;

on marine phytoplankton (Rost et al. 2008, Riebesell and Tortell 2011). By fixing CO_2 into organic matter, phytoplankton acts as a C sink and plays a potential role as a negative feedback mechanism to atmospheric pCO_2 increase (Raven and Falkowski 1999, De La Rocha and Passow 2007).

In marine ecosystems, phytoplankton productivity is often limited by availability of nitrogen (N). Fixation of atmospheric N_2 by diazotrophic cyanobacteria thus plays a crucial role for primary productivity, particularly in oligotrophic regions of the world ocean. With global change, the marine N cycle is subject to an array of perturbations. On the one hand, increasing deposition of anthropogenic N leads to eutrophication in coastal regions (Duce et al. 2008). On the other hand, the expansion of oxygen minimum zones favors N loss processes such as denitrification and anammox (Lam and Kuypers 2011). Additionally, ocean acidification is expected to decrease marine nitrification rates (Beman et al. 2011), and global warming intensifies stratification and therewith lowers nutrient input into the upper mixed layer (Doney 2006). As the latter processes are likely to decrease the overall NO_3^- availability in the surface ocean, marine N_2 fixation may become more important, helping to restore the global N budget.

The cyanobacterium *Trichodesmium* is considered one of the most important marine N_2 fixers with an estimated contribution of up to 50% to global marine N_2 fixation (Mahaffey et al. 2005). Previous studies found this diazotroph to be exceptionally sensitive to rising pCO_2. Laboratory experiments exposing cultures to pCO_2 levels projected for the end of this century showed significant increases in the production of particulate organic C and particulate organic nitrogen (POC and PON) as well as N_2 fixation rates (Barcelos é Ramos et al. 2007, Hutchins et al. 2007, 2013, Kranz et al. 2009, Levitan et al. 2007); the magnitude of these effects yet differed strongly between investigations. In several follow-up studies, CO_2 effects on *Trichodesmium* were found to be strongly modulated by other environmental factors such as iron (Shi et al. 2012) and light (Kranz et al. 2010, Levitan et al. 2010, Garcia et al. 2011), the latter highlighting the importance of energy in the modulation of CO_2 effects.

Cyanobacteria have to invest a considerable share of energy into the accumulation of inorganic carbon (C_i) by carbon concentrating mechanisms (CCMs) owing to a competing reaction with O_2 and a particularly low CO_2 affinity of their ribulose-1,5-bisphosphate carboxylase/oxygenase (RubisCO) (Badger et al. 1998). The CCM of *Trichodesmium* involves a distinct assembly of RubisCO and carbonic anhydrase (CA) within carboxysomes, as well as two C_i acquisition systems (Badger et al. 2006, Price et al. 2008). HCO_3^- is taken up via a Na^+-dependent HCO_3^- transporter (BicA) whereas diffusive uptake of CO_2 is facilitated by the so-called NDH-1_4 complex, converting CO_2 to HCO_3^-. Next to C_i acquisition, another important energy sink in *Trichodesmium* is N_2 fixation (Kranz et al. 2011). As CCM activity was found to be downregulated at high pCO_2 levels, while N_2 fixation rates were simultaneously increased in this species, a reallocation of energy between C and N_2 fixing pathways has been suggested to fuel the increase in production at high pCO_2 (Kranz et al. 2010).

Similarly to RubisCO, nitrogenase is characterized by a high sensitivity toward O_2 (Falkowski 1997). In consequence, while the fixation of N_2 is an extremely energy demanding reaction in itself (Eqn 1), diazotrophs face additional costs, which are related to the protection of nitrogenase from photosynthetically evolved O_2 (Großkopf and LaRoche 2012). To separate O_2 evolution from N_2 fixation, *Trichodesmium* has a tightly regulated diurnal cycle of N_2 fixation and photosynthesis (Berman-Frank et al. 2001), involving daily synthesis and degradation of nitrogenase (Capone et al. 1990, Sandh et al. 2009) and alternation of photosynthetic activity states (Küpper et al. 2004). Moreover, nitrogenase is expressed only in subsets of cells within filaments, the diazocytes (Lin et al. 1998, Berman-Frank et al. 2001). As no trans-cellular transport mechanisms for N compounds have been found in *Trichodesmium*, diazocytes have to release N for use by their neighboring cells (Mulholland and Capone 2000). Uptake mechanisms for N sources other than N_2 are thus indispensable for this species.

Laboratory studies have shown that *Trichodesmium* can use NO_3^- and NH_4^+ as well as organic N compounds (glutamine, glutamate or urea; Mulholland et al. 1999), all of them requiring different amounts and types of energy equivalents. NO_3^- is taken up in cyanobacteria by high-affinity ATP-dependent transporters and subsequently reduced to NH_4^+ in a two-step ferredoxin-dependent reaction catalyzed by nitrate reductase and nitrite reductase (Flores et al. 2005, Wang et al. 2000) (Eqn 2).

$$N_2 + 8\,H^+ + 8\,e^- + 16\,ATP \rightarrow 2\,NH_3 + H_2 + 16\,\left(ADP + P_i\right) \quad (1)$$

$$2\,NO_3^- + 20\,H^+ + 16\,e^- + 2\,ATP \rightarrow 2\,NH_4^+ + 6\,H_2O + 2\,\left(ADP + P_i\right) \quad (2)$$

In *Trichodesmium*, N_2 fixation was shown to be inhibited in cultures grown in NO_3^--containing media (Ohki et al. 1991, Fu and Bell 2003, Holl and Montoya 2005,

Sandh et al. 2011). As the uptake and reduction of NO_3^- requires little ATP (Eqn 2), it can be expected that NO_3^- addition to culture media will alter the energy budget of the cells in comparison to N_2 fixing conditions.

In this study, *Trichodesmium erythraeum* IMS101 was acclimated in a matrix of four different pCO_2 levels (ranging from 180 to 1400 µatm) and two different N sources (N_2 and NO_3^-). In addition to acclimation effects on the level of growth and composition (C, N and pigments), physiological key processes (N_2 fixation, O_2 fluxes and electron transport) were analyzed to improve our understanding of the plasticity in energy and resource allocation under the different energetic requirements imposed by changing environmental conditions.

Materials and methods

Culture conditions

Trichodesmium erythraeum IMS101 was grown in semi-continuous batch cultures at 25°C and 150 µmol photons $m^{-2}\,s^{-1}$ with a 12:12 h light:dark cycle. Light was provided by white fluorescent bulbs (BIOLUX, Osram, München, Germany). Cultures were grown in 0.2-µm-filtered artificial seawater (YBCII medium; Chen et al. 1996) and kept in exponential growth phase by regular dilution with culture medium. Cultures consisted of single trichomes and cell densities ranged between approximately 6000 and 180 000 cells ml^{-1}. Cells were acclimated in 1 l culture flasks, which were continuously bubbled with 0.2-µm-filtered air with pCO_2 levels of 180, 380, 980 and 1400 µatm. Gas mixtures were generated with a custom-made gas flow controller. Prior to experiments, cells were allowed to acclimate to the respective pCO_2 for at least 2 weeks. Cultures in which pH had drifted by >0.09 compared with cell-free reference media were excluded from further analysis. In treatments with NO_3^- as the N source, 0.2-µm-filtered $NaNO_3$ was added to achieve mean concentrations of 97 ± 2 µ*M* in the experiments, never falling below 65 µ*M*. Concentrations were monitored photometrically according to Collos et al. (1999). Consumption of NO_3^- by cellular uptake was compensated for by regular additions of $NaNO_3$. Cultures were acclimated to NO_3^- for at least 1 week before measurements.

Carbonate chemistry

To compensate for an increase in total alkalinity (TA) due to NO_3^- uptake (Wolf-Gladrow et al. 2007), appropriate quantities of HCl were added according to the daily changes in NO_3^- concentration. TA was determined by potentiometric titration with a TitroLine alpha plus titrator (Schott Instruments, Mainz, Germany) and calculation from linear Gran plots (Gran 1952). Average precision was ± 5 µmol kg^{-1}. Samples for dissolved inorganic carbon (DIC) analysis were filtered through 0.2 µm cellulose acetate filters and measured colorimetrically (TRAACS CS800 autoanalyzer, Seal, Norderstedt, Germany). Average precision was ± 5 µmol kg^{-1}. Certified reference materials supplied by A. Dickson (Scripps Institution of Oceanography) were used to correct for inaccuracies of TA and DIC measurements. pH values of the acclimation media were measured potentiometrically on the NBS scale [pH meter pH3110, Wissenschaftlich-Technische Werkstätten (WTW) GmbH, Weilheim, Germany]. Carbonate chemistry of the different pCO_2 and N treatments is shown in Table 1.

Growth and elemental composition

Samples for determination of growth and elemental composition of cells were generally taken between 1 and 2.5 h after beginning of the photoperiod to account for changes due to the diurnal rhythm of *Trichodesmium*. Duplicate samples for chlorophyll *a* (chl *a*) determination were extracted in acetone for >12 h and determined fluorometrically (TD-700 Fluorometer, Turner Designs, Sunnyvale, CA; Holm-Hansen and Riemann 1978). Specific growth rates (µ) were estimated by exponential regression through chl *a* concentrations measured daily over at least 4 days. Duplicate samples for analysis of POC and PON were filtered onto pre-combusted GF/F filters and stored at −20°C. Prior to analysis, filters were acidified with 200 µl HCl (0.2 *M*) to remove all inorganic C. POC and PON contents as well as PON isotopic composition ($\delta^{15}N$) were measured with an EA mass spectrometer (ANCA SL 20-20, Sercon Ltd, Crewe, UK). Daily production rates of POC and PON were obtained by multiplication of the respective elemental contents and growth rates.

N_2 fixation

N_2 fixation rates were determined using the acetylene reduction assay (ARA) (Capone 1993). Samples were spiked with acetylene (20% of head space volume) in crimp vials followed by incubation for 1 h at acclimation light and temperature with continuous agitation to avoid aggregation of cells. The amount of acetylene reduced to ethylene was then measured by gas chromatography (Trace GC, Thermo Finnigan, Bremen, Germany). Solubility of acetylene in the aqueous phase was taken into account by applying the Bunsen coefficient (0.088 at 25°C and salinity 32; Breitbarth et al. 2004). A conversion factor of 4:1 (Capone and Montoya 2001) was used to convert acetylene reduction rates to N_2 fixation rates.

Table 1. Carbonate chemistry for each pCO_2 and N treatment acquired in daily measurements during the experiment. Attained pCO_2 of the media was calculated from pH, TA, $[PO_4^{3-}]$, temperature and salinity using the CO2sys program (Pierrot et al. 2006) with equilibrium constants K_1 and K_2 given by Mehrbach et al. (1973), refit by Dickson and Millero (1987). Errors denote 1 SD ($n \geq 6$).

pCO_2 treatment (µatm)	NO_3^-	pH (NBS)	TA (µmol kg^{-1})	DIC (µmol kg^{-1})	pCO_2 attained (µatm)
180	–	8.48 ± 0.04	2415 ± 11	1847 ± 10	173 ± 12
	+	8.49 ± 0.04	2438 ± 37	1868 ± 22	168 ± 4
380	–	8.26 ± 0.03	2408 ± 15	2014 ± 6	329 ± 22
	+	8.26 ± 0.04	2389 ± 7	2003 ± 12	325 ± 10
980	–	7.88 ± 0.02	2377 ± 15	2142 ± 17	918 ± 12
	+	7.89 ± 0.03	2392 ± 19	2166 ± 26	912 ± 35
1400	–	7.74 ± 0.02	2399 ± 44	2231 ± 78	1354 ± 30
	+	7.76 ± 0.05	2413 ± 37	2237 ± 20	1298 ± 74

O_2 fluxes

Cellular O_2 fluxes were measured by means of membrane inlet mass spectrometry (MIMS) as described by Rost et al. (2007). Assays were performed in YBCII medium buffered with 4-(2-hydroxylethyl)-1-piperazine -ethanesulfonic acid (HEPES, 50 m*M*, pH 8.0) at 25°C and acclimation light intensity unless otherwise specified. To account for the diurnal cycle of O_2 fluxes in *Trichodesmium*, measurements were performed three times over the day, during time intervals from 0 to 1.5, 5.5 to 7 and 9 to 10.5 h after beginning of the photoperiod. For normalization of the O_2 traces, duplicate samples for chl *a* analysis were taken after each measurement.

In the first set of measurements, net O_2 evolution was determined as a function of DIC using the disequilibrium method described by Badger et al. (1994). O_2 fluxes were monitored during consecutive dark and light phases typically lasting 4 min, starting with DIC concentrations close to zero (media bubbled with CO_2-free air), which were subsequently increased by step-wise addition of $NaHCO_3$ up to a maximum of approximately 4500 µ*M* DIC. DIC-saturated rates of photosynthesis [V_{max} (DIC)] and half-saturation concentrations [$K_{1/2}$ (DIC)] were obtained by fitting a Michaelis–Menten function to the data.

In a second approach, O_2 evolution and uptake were assessed as a function of light intensity according to Fock and Sültemeyer (1989). Prior to measurements, HEPES-buffered YBCII media were bubbled with N_2 to remove $^{16}O_2$, then spiked with $^{18}O_2$ gas (Chemotrade, Düsseldorf, Germany) and allowed to equilibrate for >30 min, reaching O_2 concentrations of approximately 21%. DIC concentration was adjusted to approximately 2000 µ*M* by addition of 1 *M* $NaHCO_3$ solution prior to measurements. Fluxes of $^{16}O_2$ and $^{18}O_2$ were monitored during consecutive 4 min dark and light intervals, applying a range of light intensities from 8 to 2000 µmol photons m^{-2} s^{-1}. The light intensity at which photosynthesis starts to enter saturation (I_k) was obtained by a curve fit as specified by Rokitta and Rost (2012).

Fluorescence measurements

Chl *a* fluorescence was measured using the Fluorescence Induction and Relaxation (FIRe) method with a FIRe Fluorometer System (Satlantic, Halifax, Canada) and the associated actinic light source. Measurements were performed in parallel to the $^{18}O_2$ assays, following the same protocol of dark and light intervals as well as light intensities. PSII photochemical quantum yield (Fv/Fm: measured in dark-adapted state; Fv′/Fm′: measured in light-adapted state) and functional absorption cross section of PSII (σ) as well as Q_A re-oxidation time (τ) were assessed by analysis of the single turnover flash response using the Fireworx matlab code (http://sourceforge.net/projects/fireworx, written by Audrey Barnett).

Statistical analysis

Data were analyzed using R for significance of differences by two-way analysis of variance (ANOVA) tests, followed by Tukey's test for Honest Significant Differences (TukeyHSD) for specification of differences between means where appropriate. A significance level of $P \leq 0.05$ was applied.

Results

Growth and composition

Cellular chl *a* contents stayed relatively constant over the range of pCO_2 levels and N sources tested, with

a mean of 1.04 ± 0.28 pg chl *a* cell^{-1}, and were therefore used for normalization. Growth decreased slightly with increasing pCO_2 in both N treatments when all data were included (Fig. 1, ANOVA, $P < 0.005$). However, when testing CO_2 levels individually, the differences between 980 and 380 µatm as well as 180 µatm depended on the N source: with N_2 there was a significant pCO_2 effect (TukeyHSD, $adj_P < 0.05$) while with NO_3^- there was no effect (TukeyHSD, $adj_P > 0.05$). In contrast, contents of POC and PON significantly increased by approximately 33% from 180 to 1400 µatm pCO_2 (ANOVA, $P < 0.0001$). As a result of these opposing trends, production rates of POC and PON did not change over the range of pCO_2 levels tested (Table 2, ANOVA, $P > 0.05$). There was no clear trend in the pCO_2 effect on the POC:PON ratio (Table 2). Regarding effects of the N source, cells grown on NO_3^- had slightly higher growth rates than N_2 fixing cells (ANOVA, $P < 0.05$). Consequently, also production rates of POC and PON were higher in NO_3^- grown cultures (ANOVA, $P < 0.0001$), even though contents of POC and PON were not significantly affected (ANOVA, $P > 0.05$). POC:PON ratios were significantly lower in NO_3^- users than in N_2 fixers (Table 2, ANOVA, $P < 0.0001$).

N_2 fixation

N_2 fixation was inhibited by the addition of NO_3^-, with N_2 fixation rates being close to detection limit (data not shown). Moreover, the $\delta^{15}N$ of PON clearly differed between treatments (ANOVA, $P < 0.0001$), with -1.3 ± 1.0‰ in N_2 fixing cells and $+4.8 \pm 1.3$‰ in NO_3^- grown cells. N_2 fixation rates displayed a typical diurnal cycle with high rates during midday (Fig. 2). At elevated pCO_2, there was a change in the diurnal pattern toward N_2 fixation rates remaining high until the end of the photoperiod. Consequently, integrated rates of N_2 fixation over the photoperiod increased by approximately 60% from 27 to 43 nmol N_2 (µg chl *a*)$^{-1}$ day^{-1} at 380 and 1400 µatm pCO_2, respectively. At 180 and 980 µatm pCO_2, integrated rates were 25 and 39 nmol N_2 (µg chl *a*)$^{-1}$ day^{-1}, respectively.

O_2 fluxes

To characterize the energy generating processes, O_2 evolution was firstly assessed as a function of DIC concentrations. In all treatments, maximal net O_2 evolution [V_{max} (DIC)] followed a typical diurnal cycle with lowest rates during midday (Fig. 3, ANOVA, $P < 0.0001$). Values of V_{max} (DIC) were not affected by the N source or pCO_2 (ANOVA, $P > 0.5$). Half saturation concentration

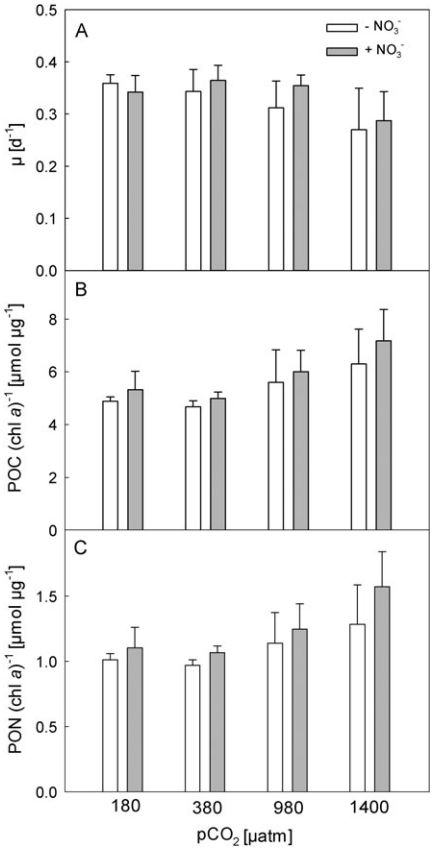

Fig. 1. Acclimation responses of *Trichodesmium* grown under different pCO_2 levels and N sources (N_2 and NO_3^-). (A) Growth rates ($n \geq 4$). (B) Ratios of POC to chl *a* ($n \geq 3$). (C) Ratios of PON to chl *a* ($n \geq 3$). Error bars denote 1 SD.

[$K_{1/2}$ (DIC)] followed a distinct diurnal pattern with significantly lower values in the morning than for the rest of the day (Fig. 3, ANOVA, $P < 0.0001$). Effects of pCO_2 on $K_{1/2}$ (DIC) were modulated by the N source and the time of day. While under NO_3^- grown conditions, there was no significant pCO_2 effect (TukeyHSD, $adj_P > 0.5$), $K_{1/2}$ (DIC) was significantly lower at 380 µatm than at 1400 µatm pCO_2 under N_2 fixing conditions (TukeyHSD, $adj_P < 0.005$). The difference between pCO_2 treatments in N_2 fixers was especially pronounced toward the evening (TukeyHSD, $adj_P < 0.0001$), with $K_{1/2}$ (DIC) decreasing in cells grown at 380 µatm but remaining high in cells grown at 1400 µatm pCO_2.

In a second approach, evolution and uptake of O_2 were assessed over a range of light intensities. Net O_2 evolution typically reached light compensation between 10 and 60 µmol photons m^{-2} s^{-1} and started to enter saturation (I_k) at approximately 280 µmol photons m^{-2} s^{-1} (Fig. 4). Light-dependent O_2 uptake, i.e. an excess of O_2 uptake in the light over O_2 uptake in the dark,

Table 2. POC and PON production and ratios of *Trichodesmium* grown under different pCO_2 levels and N sources (N_2 and NO_3^-). Errors denote 1 SD ($n \geq 3$).

pCO_2 treatment (µatm)	NO_3^-	POC production (µmol (µg chl *a*)$^{-1}$ day^{-1})	PON production (µmol (µg chl *a*)$^{-1}$ day^{-1})	POC:PON (mol:mol)
180	–	1.75 ± 0.10	0.36 ± 0.02	4.83 ± 0.10
	+	1.89 ± 0.24	0.39 ± 0.05	4.82 ± 0.06
380	–	1.60 ± 0.22	0.33 ± 0.04	4.81 ± 0.08
	+	1.82 ± 0.14	0.39 ± 0.03	4.68 ± 0.07
980	–	1.26 ± 0.42	0.26 ± 0.09	4.89 ± 0.09
	+	2.15 ± 0.19	0.45 ± 0.05	4.82 ± 0.12
1400	–	1.62 ± 0.20	0.33 ± 0.03	4.93 ± 0.21
	+	2.02 ± 0.15	0.44 ± 0.03	4.56 ± 0.07

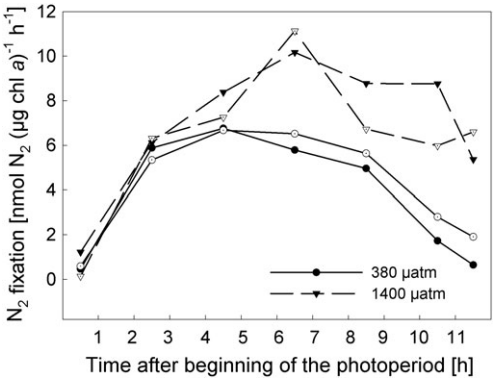

Fig. 2. Diurnal cycle of N_2 fixation in *Trichodesmium* grown at 380 µatm (circles) and 1400 µatm (triangles) pCO_2 in a 12:12 h light:dark cycle. Open and closed symbols represent biological duplicates.

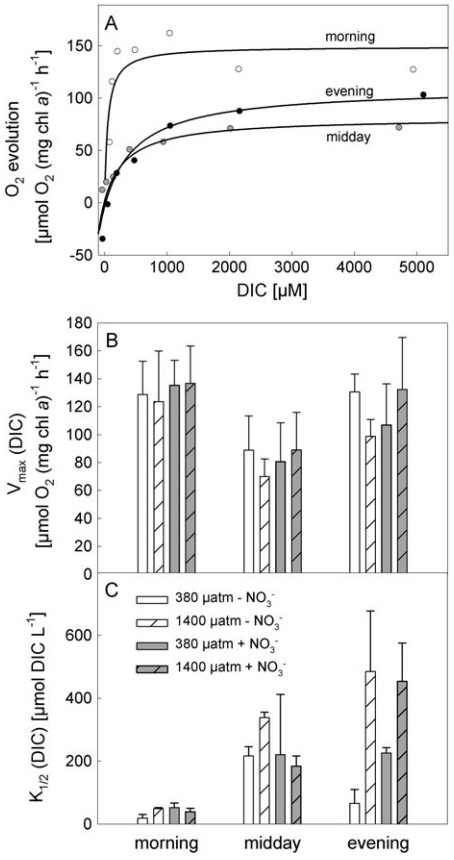

Fig. 3. Typical diurnal cycle of O_2 evolution as a function of DIC [(A) measured in *Trichodesmium* grown at 1400 µatm $-NO_3^-$]; Diurnal cycle of maximal net O_2 evolution (B) and half saturation DIC concentrations (C) in *Trichodesmium* grown under different pCO_2 levels and N sources (N_2 and NO_3^-). Error bars denote 1 SD ($n \geq 3$; except for 1400 µatm $-NO_3^-$ morning and midday and 380 µatm $+NO_3^-$ morning with $n = 2$).

was detected at irradiances >60 µmol photons m^{-2} s^{-1} (Fig. 4). Gross O_2 evolution typically saturated at higher light intensities than net photosynthesis, which is consistent with the increase in light-dependent O_2 uptake with increasing irradiance. At acclimation light intensity, diel mean values for dark respiration and light-dependent O_2 uptake amounted to 20 and 13% of gross O_2 evolution, respectively. With irradiances increasing beyond acclimation levels, light-dependent O_2 uptake increased further and equaled about 19% of gross O_2 evolution at 1300 µmol photons m^{-2} s^{-1}. Regarding effects of pCO_2 and N source on gross O_2 evolution and light-dependent O_2 uptake at acclimation light, no clear trend was found and rates followed a diurnal pattern with highest values in the morning (data not shown). Also dark respiration was not affected by pCO_2 or N source, yet rates were lowest in the morning (data not shown).

Chlorophyll fluorescence

PSII photochemical quantum yield (Fv/Fm and Fv′/Fm′) was higher at acclimation light than in the dark and decreased with increasing light intensities beyond acclimation level, covering a range between approximately 0.5 and 0.1 (Fig. 4). At low irradiances, the functional absorption cross section of PSII (σ) increased with light (by approximately 30% from approximately

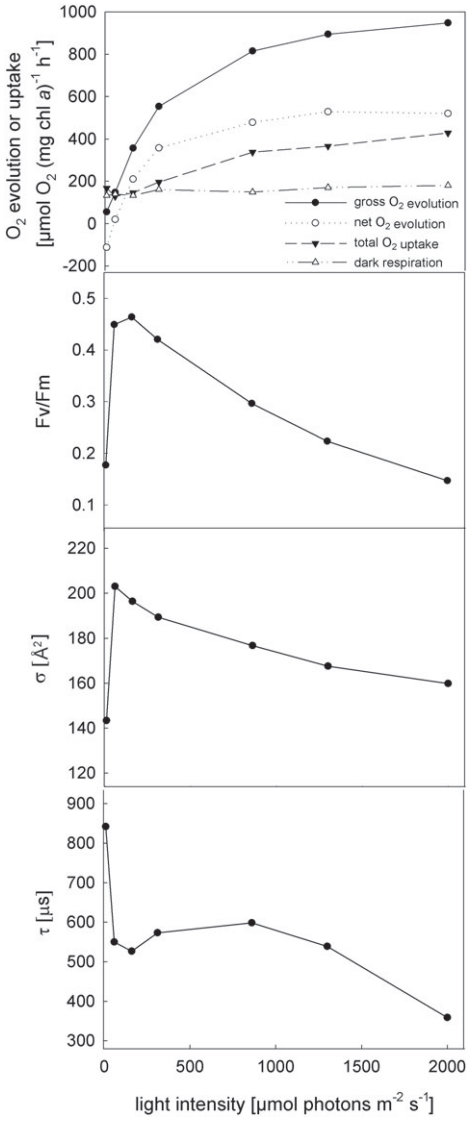

Fig. 4. Typical example of light dependence of O_2 fluxes and chlorophyll fluorescence parameters (measured in *Trichodesmium* grown at 380 µatm pCO_2 with NO_3^-). Total O_2 uptake consists of dark respiration and light-dependent O_2 uptake. Fv/Fm, PSII photochemical quantum yield; σ, PSII functional absorption cross section; τ, Q_A re-oxidation time.

8 to 60 µmol photons m^{-2} s^{-1}) while at higher light intensities, it slightly decreased (by approximately 10% from approximately 60 to 2000 µmol photons m^{-2} s^{-1}). Q_A re-oxidation time (τ) was longest in the dark and decreased by approximately 40% from approximately 60 to 2000 µmol photons m^{-2} s^{-1}.

Regarding changes in the diurnal cycle, light-adapted Fv′/Fm′ values were highest in the morning (0.48 ± 0.04 at acclimation light) and lowest at midday (0.40 ± 0.05 at acclimation light, ANOVA, $P < 0.0001$, Fig. 5). Variability over the course of the day was even more pronounced regarding dark-adapted Fv/Fm (ANOVA, $P < 0.0001$), with values ranging from 0.35 ± 0.07 (morning) to 0.17 ± 0.01 (midday). Likewise, functional absorption cross section of PSII (σ) was always highest in the morning (ANOVA, $P < 0.0001$), irrespective of light conditions. Q_A re-oxidation time, which was measured in the dark (τ_{dark}), was significantly lower in the morning than during the rest of the day (ANOVA, $P < 0.0001$), while τ_{light} decreased slightly by approximately 10% over the course of the day (ANOVA, $P < 0.05$).

Concerning responses to pCO_2 and the N source, Fv/Fm and Fv′/Fm′ were not significantly affected by either of the two parameters (Fig. 5, ANOVA, $P > 0.05$). Irrespective of light conditions, functional absorption cross section of PSII (σ) was not affected by the N source (ANOVA, $P > 0.05$), while it was slightly higher at 1400 µatm than 380 µatm pCO_2, however, only by approximately 10% (ANOVA, $P < 0.0001$). Neither τ_{dark} nor τ_{light} were significantly affected by pCO_2 or N source (ANOVA, $P > 0.5$).

Discussion

To investigate CO_2 effects on *Trichodesmium* under altered energy requirements, cultures were grown over a range of different pCO_2 levels under N_2 fixing conditions as well as with NO_3^-, the latter providing a N source with a significantly lower demand in ATP but higher electron requirements (Eqns 1 and 2). We also tested NH_4^+ as an alternative N source, which would have altered the energy requirements most strongly, lowering the ATP as well as the electron demand compared with N_2 fixation. However, measurements revealed NH_4^+ to be toxic to *Trichodesmium* in concentrations as low as 10 µ*M* (data not shown), which equaled the average daily N consumption in our cultures, and therefore argued against the applicability in dilute batch incubations. Additionally, concentrations could not be kept stable because of pH-dependent out-gassing of NH_3 (data not shown), rendering it impossible to perform pCO_2 manipulations without simultaneously affecting the N availability. The addition of NO_3^-, on the other hand, had no negative effects on *Trichodesmium* and was not influenced by pH. As a consequence, we chose NO_3^- to impose a change in the energy status of cells. The change in N usage upon NO_3^- addition was demonstrated by direct measurements of nitrogenase activity as well as by the change in ^{15}N composition of PON. NO_3^- assimilation resulted in corresponding changes in TA, which were compensated by additions of HCl in equimolar amounts to keep the carbonate system comparable between N_2 fixing and NO_3^- using cultures. Growth rates and Fv/Fm indicate that cells were not stressed in any of the treatments.

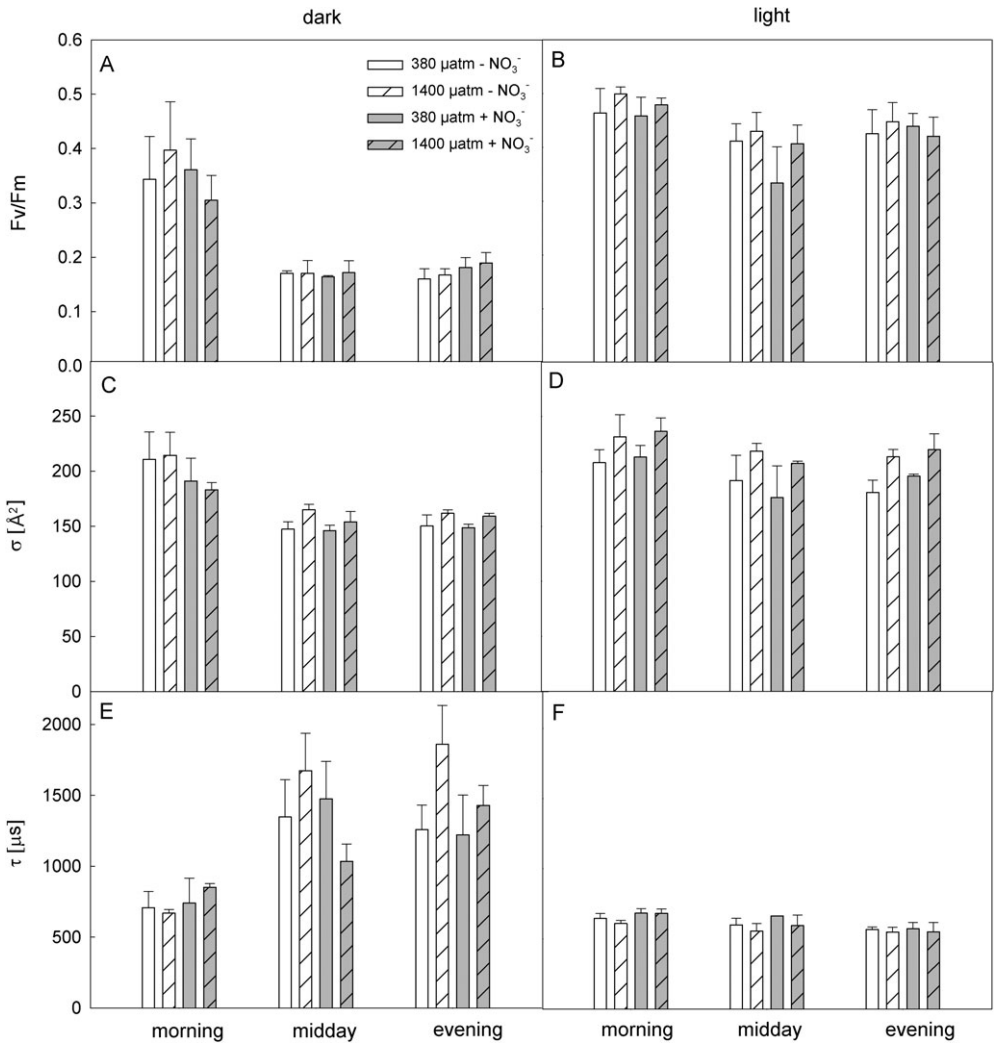

Fig. 5. Diurnal cycle of chlorophyll fluorescence of *Trichodesmium* cultures grown under different pCO_2 levels and N sources (N_2 and NO_3^-), measured in the dark (A, C and E) and at acclimation light intensity (B, D and F). Error bars denote 1 SD ($n \geq 3$, except for τ of 380 µatm +NO_3^- midday with $n = 1$). Fv/Fm, PSII photochemical quantum yield; σ, PSII functional absorption cross section; τ, Q_A re-oxidation time.

Please note that the light level applied in the acclimations (150 µmol photons m^{-2} s^{-1}) was below saturation (Fig. 4), imposing a general energy constraint in the cell.

Acclimation effects of different pCO_2 levels and N sources

The increase of POC as well as PON with pCO_2 (Fig. 1) is in accordance with previous results (Kranz et al. 2009, 2010). Respective production rates, however, stayed relatively constant due to the concomitant decrease in growth (Table 2, Fig. 1). In other words, cells contained less biomass and divided more quickly at low and medium pCO_2, while at high pCO_2, cell quotas were higher and cells divided more slowly. Among the previous studies on *T. erythraeum* IMS101 testing the effect of pCO_2 levels up to 750 or 1000 µatm, some showed an increase in growth rate with pCO_2 (Barcelos é Ramos et al. 2007, Levitan et al. 2007, Kranz et al. 2010, Garcia et al. 2011), while others did not find significant differences (Hutchins et al. 2007, Kranz et al. 2009). Only one study has tested CO_2 levels comparable to our highest CO_2 treatment, finding that positive effects on growth leveled off between 760 and 1500 µatm in *T. erythraeum* GBRTRL101 (Hutchins et al. 2007). In a recent study investigating pCO_2 effects under low iron availability representative for oligotrophic oceans, growth rates of *Trichodesmium* were shown to decrease with pCO_2 (380 vs 750 µatm; Shi et al. 2012).

The stimulation in PON production in NO_3^- grown cells may be directly attributed to the lower energy requirement for N assimilation (Table 2, Eqns 1 and 2) as well as the fact that filaments are not subject to N loss during transfer from diazocytes to non-diazotrophic cells when grown on NO_3^-. The effect on POC production, however, cannot be directly linked to N assimilation and suggests a more global effect of NO_3^- on the cells' metabolism such as reallocation of energy from N to C assimilation. The cost reduction associated with the switch from N_2 to NO_3^- assimilation is also reflected in the lower POC:PON ratios under these conditions (Table 2). Changes in POC:PON ratios have been found in response to nutrient limitation in different phytoplankton (Sterner and Elser 2002). Even though none of our treatments was N limited, the observed changes in POC:PON ratios may simply reflect the higher N assimilation costs in N_2 fixers.

O_2 fluxes and electron transport

To better understand how the observed effects of pCO_2 and N source on POC and PON were fuelled, we investigated photosynthesis as a measure of energy generation. Concerning treatment effects, neither pCO_2 nor the N source had a significant effect on net O_2 evolution (Fig. 3). However, net O_2 evolution can be uncoupled from energy generation by high rates of O_2 uptake or cyclic electron transport (Heber 2002). Thus, gross and net O_2 fluxes as well as chlorophyll fluorescence need to be considered to obtain a more complete picture of energy generating processes. In all cultures, irrespective of pCO_2 or N source, about one third of the gross O_2 evolved was consumed by dark respiration and light-dependent O_2 uptake (Fig. 4), the latter being indicative for either the classical Mehler reaction (Mehler 1951) or the equivalent reduction of O_2 by flavoproteins (Helman et al. 2003). High rates of O_2 uptake by dark respiration and Mehler reaction have been suggested to protect nitrogenase from O_2 inhibition in *Trichodesmium* (Kana 1993, Carpenter and Roenneberg 1995, Berman-Frank et al. 2001, Milligan et al. 2007). Rates of Mehler reaction equaled only about 10% of gross O_2 evolution at acclimation light intensity, yet rates increased when light intensities exceeded acclimation levels (Fig. 4). This light dependency could either indicate a role for Mehler reaction in photoprotection and/or reflect the enhanced need for nitrogenase protection at high gross O_2 evolution rates. Moreover, the fact that light-dependent O_2 uptake was not significantly affected by the N source seems surprising, considering the proposed role of Mehler reaction in nitrogenase protection in *Trichodesmium* (Milligan et al. 2007).

Chlorophyll fluorescence showed a light response typical for cyanobacteria, with dark-adapted fluorescence being controlled by respiratory electron flow that introduces electrons into the plastoquinone (PQ) pool (reviewed by Campbell et al. 1998). At low light intensities, electron flux through PSI is induced, oxidizing the PQ pool and thereby increasing Fv′/Fm′ and decreasing Q_A re-oxidation time (τ) (Fig. 4). When light intensities increase beyond acclimation light, input of excitation energy can become higher than the cells' capacity of ferredoxin re-oxidation, making cells vulnerable to photodamage. However, being adapted to high and variable light regimes, *Trichodesmium* employs effective photoprotective mechanisms (Breitbarth et al. 2008, Andresen et al. 2009). First of all, state transitions lead to a re-arrangement of phycobilisomes toward PSI, decreasing the PSII functional absorption cross section (σ) and therewith Fv′/Fm′ (Fig. 4). Second, the enhanced rates of Mehler reaction dissipate electrons at high light (Fig. 4). The effectiveness of these photoprotective mechanisms is reflected in a decreasing Q_A re-oxidation time (τ) whilst gross O_2 evolution increases with light (Fig. 4).

To cover the high ATP demand of N_2 fixation (Table 3; Eqn 1), *Trichodesmium* depends on high rates of cyclic electron transport and Mehler reaction, increasing the ATP:NADPH ratio beyond that provided by linear photosynthetic electron transport. High rates of cyclic electron transport have been proposed to result in chemical reduction of the PQ pool, increasing re-oxidation time of Q_A (Berman-Frank et al. 2001). Assuming that cells adjust their energy generation closely to their needs, we expected the treatment-dependent differences in energy demand to be reflected in chlorophyll fluorescence. Contrary to our assumption, none of the fluorescence parameters measured was affected by pCO_2 or N source with the exception of a small pCO_2 effect on functional absorption cross section of PSII (σ, Fig. 5).

Regarding the diurnal cycle, there was a characteristic downregulation of maximal net photosynthesis as well as Fv/Fm during midday, which has been shown previously in *Trichodesmium* as part of the cells' mechanisms to reduce O_2 concentrations during the phase of highest N_2 fixation (Berman-Frank et al. 2001). In the morning, highly efficient electron transport was indicated by high Fv/Fm and a large PSII functional absorption cross section (Fig. 5), which is in line with the high gross O_2 evolution (data not shown). Dark respiration, as indicated by τ_{dark} and O_2 flux measurements, was lowest in the morning, while rates of Mehler reaction were at their maximum. Later during the day, rates of photosynthetic electron transport decreased, reflected by lower Fv/Fm, functional absorption cross section of PSII (σ), O_2

Table 3. Theoretical ATP and electron (e^-) costs of cellular processes and costs calculated for the observed POC and PON production rates under two different N sources (N_2 and NO_3^-). Theoretical demands of C fixation, CCM and POC production were normalized to mol N using the average POC:PON ratio measured in the experiment. CCM costs are based on 80% HCO_3^- use and a transport cost of 0.5 mol ATP per mol HCO_3^-, assuming 50% CO_2 leakage. Costs of NO_3^- assimilation include 1 mol ATP for uptake. Loss of fixed nitrogen (e.g. NH_4^+) is not accounted for. Please note that numbers given do not include costs for synthesis of enzymes and transporters, which would significantly increase the estimates for fixation of carbon as well as nitrogen (Brown et al. 2008). POM (particulate organic matter) is the sum of POC and PON.

Process	Unit	ATP	e^-	ATP:NADPH + H^+	Reference
C fixation	mol (mol N)$^{-1}$	14	19	1.5	Allen 2002
CCM	mol (mol N)$^{-1}$	4	0		Hopkinson et al. 2011
POC production	mol (mol N)$^{-1}$	18	19	1.9	
N_2 assimilation to NH_4^+	mol (mol N)$^{-1}$	8	4	4.0	Flores and Herrero 1994
NO_3^- assimilation to NH_4^+	mol (mol N)$^{-1}$	1	8	0.3	Flores et al. 2005
NH_4^+ assimilation to glutamate	mol (mol N)$^{-1}$	1	2	1.0	Flores et al. 2005
PON production N_2 fixer	mol (mol N)$^{-1}$	9	6	3.0	
PON production NO_3^- user	mol (mol N)$^{-1}$	2	10	0.4	
POC production measured in N_2 fixer	μmol (μg chl a)$^{-1}$ day^{-1}	5.9	6.2	1.9	
POC production measured in NO_3^- user	μmol (μg chl a)$^{-1}$ day^{-1}	7.5	7.9	1.9	
POC production difference NO_3^- vs N_2	μmol (μg chl a)$^{-1}$ day^{-1}	1.6	1.7		
PON production measured in N_2 fixer	μmol (μg chl a)$^{-1}$ day^{-1}	2.9	1.9	3.0	
PON production measured in NO_3^- user	μmol (μg chl a)$^{-1}$ day^{-1}	0.8	4.2	0.4	
PON production difference NO_3^- vs N_2	μmol (μg chl a)$^{-1}$ day^{-1}	−2.0	2.3		
Total POM production in N_2 fixer	μmol (μg chl a)$^{-1}$ day^{-1}	8.8	8.2	2.2	
Total POM production in NO_3^- user	μmol (μg chl a)$^{-1}$ day^{-1}	8.3	12.1	1.4	
POM production difference NO_3^- vs N_2	μmol (μg chl a)$^{-1}$ day^{-1}	−0.5	3.9		

evolution as well as Mehler reaction, while dark respiration increased. Interestingly, the diurnal cycle of O_2 evolution and uptake as well as electron transport was maintained also in NO_3^- grown cultures. Studies on the diurnal cycle of nitrogenase protein abundance in *Trichodesmium* showed that nitrogenase is synthesized de novo every day (Zehr et al. 1996), resulting in a significant energy demand for protein synthesis (Brown et al. 2008). Nitrogenase was found to be synthesized, yet not activated by post-translational modification, in cells grown even at high levels of NO_3^- (Ohki et al. 1991). These findings suggest that although nitrogenase was not active, NO_3^- grown cells in our study may still have invested a considerable amount of energy for synthesis of nitrogenase. This would cause similar energy requirements as well as protection of nitrogenase from O_2 also in NO_3^- grown cells (i.e. O_2 consumption by dark respiration and Mehler reaction as well as downregulation of photosynthesis during midday), explaining the lack of N effects on chlorophyll fluorescence and O_2 fluxes observed in our study. There is, however, also data suggesting significantly lower expression levels of nitrogenase subunits NifK and NifH in NO_3^- grown cells (Sandh et al. 2011).

In summary, the lack of a clear pCO_2 or N effect on photosynthesis, dark respiration or Mehler reaction confirms that there was no difference in energy generation (ATP and reducing equivalents). The observed treatment effects on contents and production of POC and PON can thus not be explained by differences in the overall energy availability, indicating potential changes down-stream of the electron transport chain. To identify alterations in the energy consuming processes we therefore measured rates of N_2 fixation and C acquisition.

N_2 fixation

In agreement with previous results (Kranz et al. 2010), a characteristic change in the diurnal pattern of N_2 fixation was observed at elevated pCO_2, with the phase of high nitrogenase activity being prolonged toward the evening (Fig. 2). Although integrated daily N_2 fixation rates increased by as much as 60% between 380 and 1400 μatm pCO_2, PON production was not significantly affected by the different pCO_2 levels. The ARA used for estimating N_2 fixation rates gives a measure of the maximal nitrogenase enzyme activity under the respective assay conditions (approximating gross N_2 fixation) while PON production rates reflect how much N is ultimately incorporated into the cells (approximating net N_2 fixation). While there are indications that a considerable share of fixed N is lost before incorporation into PON (Mulholland and Capone 2000, Mulholland 2007), significant uncertainties remain with respect to the absolute values due to methodological issues (Mulholland and Capone 2001 and references therein). It also has to be noted that, in contrast to acetylene reduction during ARA, actual N_2 fixation is dependent on ammonium consumption by downstream metabolism (e.g. Herrero et al.

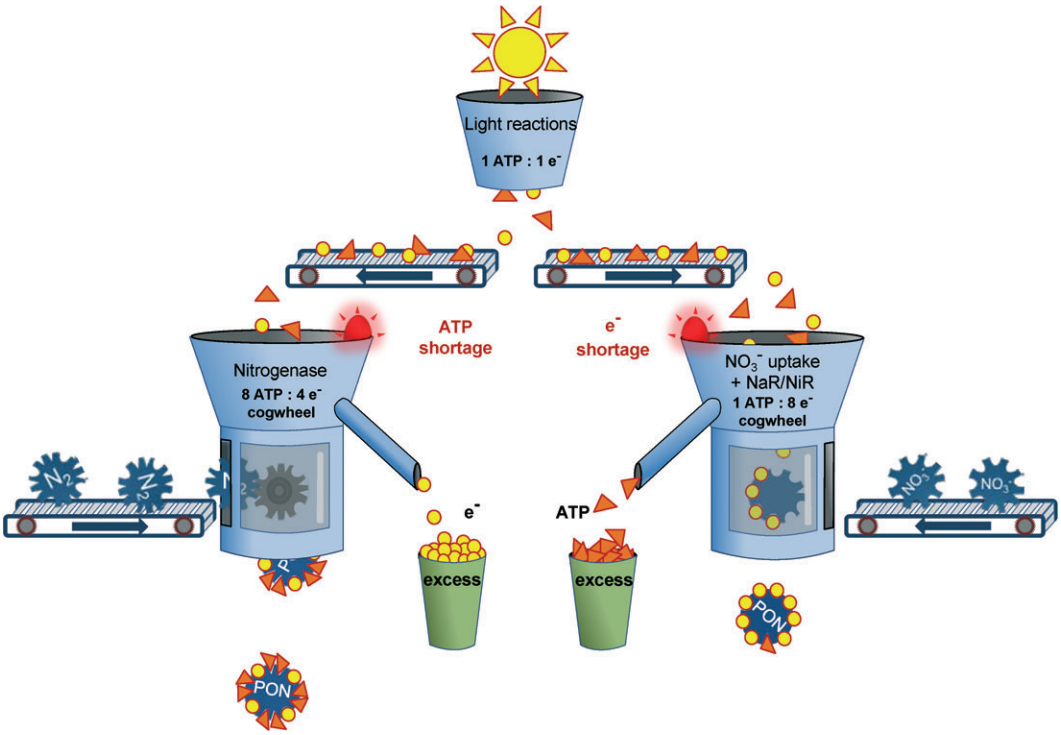

Fig. 6. Schematic diagram of the distribution of energy equivalents for PON production under different N sources (N_2 and NO_3^-). Due to the different requirements of N_2 and NO_3^- assimilation with respect to ATP and electron (e^-) stoichiometry, N_2 fixation is prone to limitation by ATP while NO_3^- assimilation tends to be limited by e^- supply. Please note that the ultimate outcome in terms of PON production in the different N treatments is strongly dependent on the ratio of ATP per e^- available, which is, in turn, controlled by the ratio of (pseudo-) cyclic to linear e^- transport and the use of energy equivalents by other cellular processes. NaR, nitrate reductase; NiR, nitrite reductase.

2001). However, interpretation of trends within results of each of the methods should be valid. In accordance with our findings on CO_2 sensitivity, previous studies found ARA-based estimates of N_2 fixation to increase more strongly with pCO_2 than estimates of PON production based on cell quotas or ^{15}N fixation (Kranz et al. 2010, Garcia et al. 2011). In the natural environment, N release by *Trichodesmium* has been suggested to provide an important N source for a range of associated organisms (Mulholland and Capone 2000, Mulholland 2007), which may be enhanced under elevated pCO_2 according to our data. The high assimilation costs and unavoidable N loss in N_2 fixers impose higher energy requirements compared with NO_3^- users, especially under elevated pCO_2. As all treatments, however, showed the same energy generation, we expect changes in other energy sinks.

Inorganic C acquisition

Acquisition of inorganic C constitutes a major energy sink in *Trichodesmium* due to the high CCM activities required to compensate for the poor CO_2 affinity of its RubisCO (Kranz et al. 2009). Similarly to O_2 and electron fluxes as well as N_2 fixation, also the affinity for inorganic C was subject to a strong diurnal cycle (Fig. 3), which was previously described by Kranz et al. (2009). The high affinity for inorganic C in the mornings observed in all treatments is in line with the high rates of photosynthesis discussed above. The overall lower affinities at high pCO_2, especially during the second half of the day, suggest significantly lower operational costs for the CCM which, in turn, allow for the enhanced N_2 fixation observed (Figs 2 and 3). These CO_2-dependent changes in affinities and the anti-correlation with N_2 fixation are in agreement with previous results (Kranz et al. 2010). The fact that pCO_2 effects are larger in N_2 fixers than in NO_3^- using cells can be attributed to the higher overall energy requirements of N_2 fixation as well as differences in the stoichiometry of ATP and electron demand (Fig. 6): Provided that the downregulation of CCM activity mainly saves ATP, this surplus energy can be readily used in N_2 fixers to cover the high ATP demand of nitrogenase. In contrast, NO_3^- usage requires only little ATP (for uptake) and is, instead, likely to be limited by the supply of reducing equivalents. Consequently, a downregulation of the

CCM in NO_3^- users would not have the same stimulatory effect on PON production as in N_2 fixers.

Energy requirements of the CCM are generally dependent on the C sources and uptake mechanisms. CCM operation in *Trichodesmium* is considered to predominantly consume ATP, as the main C source for this species is HCO_3^- (approximately 80%; Kranz et al. 2009, 2010), which is taken up via a transporter fuelled indirectly by ATP (BicA; Price et al. 2008). Such HCO_3^- transporters are dependent on a Na^+ gradient across the plasma membrane and presumably consume 0.5 mol ATP per mol HCO_3^- (Espie and Kandasamy 1994, Hopkinson et al. 2011). Furthermore, the so-called NDH-1_4 complex converts CO_2 to HCO_3^-, thereby driving uptake of CO_2 as well as an internal recycling to prevent CO_2 leakage (Price et al. 2002, 2008). The reaction is involved in the electron transport chain, receiving electrons from NADPH or ferredoxin that are subsequently transferred to PQ. Intriguingly, NDH-1_4 activity leads to a release of protons into the thylakoid lumen, which in turn increases the pH gradient used for ATP synthesis. The observation that this complex seems to be especially active at high pCO_2 (Kranz et al. 2010) is in line with the increased ATP demand by enhanced N_2 fixation under these conditions (Fig. 2). It has to be noted that the operational costs for BicA and NDH-1_4 are still under debate. Provided that the two CCM components have opposing effects on cellular ATP levels, it is crucial to investigate their differential regulation in response to different environmental conditions.

Conclusions

Despite the change in energy demand imposed by the different pCO_2 levels and N sources, *Trichodesmium* showed no alteration in energy producing pathways. Yet, elevated pCO_2 increased cellular POC and PON contents in both N treatments. In N_2 fixers, also nitrogenase activity was strongly enhanced with pCO_2. Concurrently, CCM activity was downregulated, reducing the use of ATP in active HCO_3^- uptake and allowing its allocation to N_2 fixation. The increase in N_2 fixation was, however, not reflected in PON production, possibly due to an increase in N loss with increasing pCO_2. In NO_3^- users, the lower N-normalized ATP demand for PON production (Table 3) and the better N retention allowed for higher production rates of POC as well as PON compared with N_2 fixers. A calculation of the theoretical energy demands of the measured POC and PON production rates (Table 3) revealed that most of the ATP saved from the switch to NO_3^- use (approximately 80%) was invested into increasing the production rates of POC and PON, resulting in almost unaltered ATP demand in our cultures (0.5 ATP residue, Table 3). The concomitant increase in the demand of reducing equivalents may have prevented a full implementation of ATP savings into the production of particulate organic matter (POM). The effects of pCO_2 on CCM activity were smaller in NO_3^- users than in N_2 fixers, highlighting the dependence of energy reallocation on the stoichiometric demands in energy equivalents: As NO_3^- assimilation requires only little ATP and is limited by electrons (Fig. 6), any spare ATP arising from downregulation of the CCM would not have the same stimulatory effect as in N_2 fixers. Interestingly, the diurnal pattern in O_2 fluxes usually attributed to protection of nitrogenase was maintained also in NO_3^- grown cells. Further studies are necessary to unravel the effects of different environmental conditions on cellular energy budgets, focusing on energization of the CCM as well as the intricate effects of the NDH-1_4 complex on C use efficiency and energy balance.

Author contributions

M. E., S. A. K. and B. R. conceived and designed the experiment. M. E. and S. A. K. performed the experiments. M. E. analyzed the data; M. E., S. A. K. and B. R. wrote the paper.

Acknowledgements – We thank Ulrike Richter, Jana Hölscher and Klaus-Uwe Richter for laboratory assistance and technical support. Grant support was provided by the European Research Council under the European Community's Seventh Framework Programme (FP7/2007-2013)/ERC grant agreement (205150).

References

Allen JF (2002) Photosynthesis of ATP – electrons, proton pumps, rotors, and poise. Cell 110: 273–276

Andresen E, Lohscheider J, Setlikova E, Adamska I, Simek M, Kupper H (2009) Acclimation of *Trichodesmium erythraeum* IMS101 to high and low irradiance analysed on the physiological, biophysical and biochemical level. New Phytol 185: 173–188

Badger MR, Palmqvist K, Yu JW (1994) Measurement of CO_2 and HCO_3^- fluxes in cyanobacteria and microalgae during steady-state photosynthesis. Physiol Plant 90: 529–536

Badger MR, Andrews TJ, Whitney SM, Ludwig M, Yellowlees DC (1998) The diversity and co-evolution of Rubisco, plastids, pyrenoids and chloroplast-based CO_2-concentrating mechanisms in algae. Can J Bot 76: 1052–1071

Badger MR, Price GD, Long BM, Woodger FJ (2006) The environmental plasticity and ecological genomics of the cyanobacterial CO_2 concentrating mechanism. J Exp Bot 57: 249–265

Barcelos é Ramos J, Biswas H, Schulz KG, LaRoche J, Riebesell U (2007) Effect of rising atmospheric carbon dioxide on the marine nitrogen fixer *Trichodesmium*. Global Biogeochem Cycles 21. DOI: 10.1029/2006GB002898

Beman JM, Chow CE, King AL, Feng YY, Fuhrman JA, Andersson A, Bates NR, Popp BN, Hutchins DA (2011) Global declines in oceanic nitrification rates as a consequence of ocean acidification. Proc Natl Acad Sci USA 108: 208–213

Berman-Frank I, Lundgren P, Chen YB, Kupper H, Kolber Z, Bergman B, Falkowski P (2001) Segregation of nitrogen fixation and oxygenic photosynthesis in the marine cyanobacterium *Trichodesmium*. Science 294: 1534–1537

Breitbarth E, Mills MM, Friedrichs G, LaRoche J (2004) The Bunsen gas solubility coefficient of ethylene as a function of temperature and salinity and its importance for nitrogen fixation assays. Limnol Oceanogr Methods 2: 282–288

Breitbarth E, Wohlers J, Kläs J, LaRoche J, Peeken I (2008) Nitrogen fixation and growth rates of *Trichodesmium* IMS-101 as a function of light intensity. Mar Ecol Prog Ser 359: 25–36

Brown CM, MacKinnon JD, Cockshutt AM, Villareal TA, Campbell DA (2008) Flux capacities and acclimation costs in *Trichodesmium* from the Gulf of Mexico. Mar Biol 154: 413–422

Caldeira K, Wickett ME (2003) Anthropogenic carbon and ocean pH. Nature 425: 365

Campbell D, Hurry V, Clarke AK, Gustafsson P, Öquist G (1998) Chlorophyll fluorescence analysis of cyanobacterial photosynthesis and acclimation. Microbiol Mol Biol Rev 62: 667–683

Capone DG (1993) Determination of nitrogenase activity in aquatic samples using the acetylene reduction procedure. In: Kemp PF, Sherr B, Sherr E, Cole J (eds) Handbook of Methods in Aquatic Microbial Ecology. Lewis Publishers, New York, pp 621–631

Capone DG, Montoya JP (2001) Nitrogen fixation and denitrification. Methods Microbiol 30: 501–515

Capone DG, Oneil JM, Zehr J, Carpenter EJ (1990) Basis for diel variation in nitrogenase activity in the marine planktonic cyanobacterium *Trichodesmium thiebautii*. Appl Environ Microbiol 56: 3532–3536

Carpenter EJ, Roenneberg T (1995) The marine planktonic cyanobacteria *Trichodesmium* spp – photosynthetic rate measurements in the SW Atlantic Ocean. Mar Ecol Prog Ser 118: 267–273

Chen YB, Zehr JP, Mellon M (1996) Growth and nitrogen fixation of the diazotrophic filamentous nonheterocystous cyanobacterium *Trichodesmium* sp. IMS 101 in defined media: evidence for a circadian rhythm. J Phycol 32: 916–923

Collos Y, Mornet F, Sciandra A, Waser N, Larson A, Harrison PJ (1999) An optical method for the rapid measurement of micromolar concentrations of nitrate in marine phytoplankton cultures. J Appl Phycol 11: 179–184

De La Rocha CL, Passow U (2007) Factors influencing the sinking of POC and the efficiency of the biological carbon pump. Deep Sea Res Part II Top Stud Oceanogr 54: 639–658

Dickson AG, Millero FJ (1987) A comparison of the equilibrium constants for the dissociation of carbonic acid in seawater media. Deep Sea Res 34: 1733–1743

Doney SC (2006) Oceanography – Plankton in a warmer world. Nature 444: 695–696

Duce RA, LaRoche J, Altieri K, Arrigo KR, Baker AR, Capone DG, Cornell S, Dentener F, Galloway J, Ganeshram RS, Geider RJ, Jickells T, Kuypers MM, Langlois R, Liss PS, Liu SM, Middelburg JJ, Moore CM, Nickovic S, Oschlies A, Pedersen T, Prospero J, Schlitzer R, Seitzinger S, Sorensen LL, Uematsu M, Ulloa O, Voss M, Ward B, Zamora L (2008) Impacts of atmospheric anthropogenic nitrogen on the open ocean. Science 320: 893–897

Espie GS, Kandasamy RA (1994) Monensin inhibition of Na^+-dependent HCO_3^- transport distinguishes it from Na^+-independent HCO_3^- transport and provides evidence for Na^+/HCO_3^- symport in the cyanobacterium *Synechococcus* UTEX-625. Plant Physiol 104: 1419–1428

Falkowski PG (1997) Evolution of the nitrogen cycle and its influence on the biological sequestration of CO_2 in the ocean. Nature 387: 272–275

Flores E, Herrero A (1994) Assimilatory nitrogen metabolism and its regulation. In: Bryant DA (ed) The Molecular Biology of Cyanobacteria. Kluwer Academic Publishers, Dordrecht, pp 487–517

Flores E, Frias JE, Rubio LM, Herrero A (2005) Photosynthetic nitrate assimilation in cyanobacteria. Photosynth Res 83: 117–133

Fock HP, Sültemeyer DF (1989) O_2 evolution and uptake measurements in plant cells by mass spectrometer. In: Liskens HF, Jackson JF (eds) Modern Methods of Plant Analysis, Vol. 9. Springer-Verlag, Heidelberg, pp 3–18

Fu FX, Bell PRF (2003) Factors affecting N_2 fixation by the cyanobacterium *Trichodesmium* sp GBR-TRLI101. FEMS Microbiol Ecol 45: 203–209

Garcia NS, Fu FX, Breene CL, Bernhardt PW, Mulholland MR, Sohm JA, Hutchins DA (2011) Interactive effects of light and CO_2 on CO_2 fixation and N_2 fixation in the diazotroph *Trichodesmium erythraeum* (cyanobacteria). J Phycol 47: 1292–1303

Gran G (1952) Determination of the equivalence point in potentiometric titrations. Part II. Analyst 77: 661–671
Großkopf T, LaRoche J (2012) Direct and indirect costs of dinitrogen fixation in *Crocosphaera watsonii* WH8501 and possible implications for the nitrogen cycle. Front Microbiol 3: 236
Heber U (2002) Irrungen, Wirrungen? The Mehler reaction in relation to cyclic electron transport in C3 plants. Photosynth Res 73: 223–231
Helman Y, Tchernov D, Reinhold L, Shibata M, Ogawa T, Schwarz R, Ohad I, Kaplan A (2003) Genes encoding A-type flavoproteins are essential for photoreduction of O_2 in cyanobacteria. Curr Biol 13: 230–235
Herrero A, Muro-Pastor AM, Flores E (2001) Nitrogen control in cyanobacteria. J Bacteriol 183: 411–425
Holl CM, Montoya JP (2005) Interactions between nitrate uptake and nitrogen fixation in continuous cultures of the marine diazotroph *Trichodesmium* (Cyanobacteria). J Phycol 41: 1178–1183
Holm-Hansen O, Riemann B (1978) Chlorophyll a determination: improvements in methodology. Oikos 30: 438–447
Hopkinson BM, Dupont CL, Allen AE, Morel FM (2011) Efficiency of the CO_2-concentrating mechanism of diatoms. Proc Natl Acad Sci USA 108: 3830–3837
Hutchins DA, Fu F-X, Zhang Y, Warner ME, Feng Y, Portune K, Bernhardt PW, Mulholland MR (2007) CO_2 control of *Trichodesmium* N_2 fixation, photosynthesis, growth rates and elemental ratios: implications for past, present and future ocean biogeochemistry. Limnol Oceanogr 552: 1293–1304
IPCC (2007) Summary for policymakers. In: Solomon S, Qin D, Manning M, Chen Z, Marquis M, Averyt KB, Tignor M, Miller HL (eds) Climate Change 2007: The Physical Science Basis. Contribution of Working Group I to the Fourth Assessment Report of the Intergovernmental Panel on Climate Change. Cambridge University Press, Cambridge
Kana TM (1993) Rapid oxygen cycling in *Trichodesmium thiebautii*. Limnol Oceanogr 38: 18–24
Kranz SA, Sültemeyer D, Richter KU, Rost B (2009) Carbon acquisition in *Trichodesmium*: the effect of pCO_2 and diurnal changes. Limnol Oceanogr 54: 548–559
Kranz SA, Levitan O, Richter KU, Prasil O, Berman-Frank I, Rost B (2010) Combined effects of CO_2 and light on the N_2 fixing cyanobacterium *Trichodesmium* IMS101: Physiological responses. Plant Physiol 154: 334–345
Kranz SA, Eichner M, Rost B (2011) Interactions between CCM and N_2 fixation in *Trichodesmium*. Photosynth Res 109: 73–84
Küpper H, Ferimazova N, Setlik I, Berman-Frank I (2004) Traffic lights in *Trichodesmium*. Regulation of photosynthesis for nitrogen fixation studied by chlorophyll fluorescence kinetic microscopy. Plant Physiol 135: 2120–2133
Lam P, Kuypers MMM (2011) Microbial nitrogen cycling processes in oxygen minimum zones. Annu Rev Mar Sci 3: 317–345
Levitan O, Rosenberg G, Setlik I, Setlikova E, Grigel J, Klepetar J, Prasil O, Berman-Frank I (2007) Elevated CO_2 enhances nitrogen fixation and growth in the marine cyanobacterium *Trichodesmium*. Glob Chang Biol 13: 531–538
Levitan O, Kranz SA, Spungin D, Prasil O, Rost B, Berman-Frank I (2010) The combined effects of CO_2 and light on the N_2 fixing cyanobacterium *Trichodesmium* IMS101: a mechanistic view. Plant Physiol 154: 346–356
Lin SJ, Henze S, Lundgren P, Bergman B, Carpenter EJ (1998) Whole-cell immunolocalization of nitrogenase in marine diazotrophic cyanobacteria, *Trichodesmium* spp. Appl Environ Microbiol 64: 3052–3058
Mahaffey C, Michaels AF, Capone DG (2005) The conundrum of marine N_2 fixation. Am J Sci 305: 546–595
Mehler AH (1951) Studies on reactions of illuminated chloroplasts. I. Mechanism of the reduction of oxygen and other Hill reagents. Arch Biochem Biophys 33: 65–77
Mehrbach C, Culberson CH, Hawley JE, Pytkowicz RM (1973) Measurement of the apparent dissociation constants of carbonic acid in seawater at atmospheric pressure. Limnol Oceanogr 18: 897–907
Milligan AJ, Berman-Frank I, Gerchman Y, Dismukes GC, Falkowski PG (2007) Light-dependent oxygen consumption in nitrogen-fixing cyanobacteria plays a key role in nitrogenase protection. J Phycol 43: 845–852
Mulholland MR (2007) The fate of nitrogen fixed by diazotrophs in the ocean. Biogeosciences 4: 37–51
Mulholland MR, Capone DG (2000) The nitrogen physiology of the marine N_2-fixing cyanobacteria *Trichodesmium* spp. Trends Plant Sci 5: 148–153
Mulholland MR, Capone DG (2001) Stoichiometry of nitrogen and carbon utilization in cultured populations of *Trichodesmium* IMS101: implications for growth. Limnol Oceanogr 46: 436–443
Mulholland MR, Ohki K, Capone DG (1999) Nitrogen utilization and metabolism relative to patterns of N_2 fixation in cultures of *Trichodesmium* NIBB1067. J Phycol 35: 977–988
Ohki K, Zehr JP, Falkowski PG, Fujita Y (1991) Regulation of nitrogen-fixation by different nitrogen-sources in the marine nonheterocystous cyanobacterium *Trichodesmium* sp NIBB1067. Arch Microbiol 156: 335–337
Pierrot D, Lewis E, Wallace D (2006) MS Excel program developed for CO_2 system calculations. ORNL/CDIAC-105. Carbon Dioxide Information Analysis Center, Oak Ridge National Laboratory, US Department of Energy, Oak Ridge, TN

Price GD, Maeda S, Omata T, Badger MR (2002) Modes of inorganic carbon uptake in the cyanobacterium *Synechococcus* sp. PCC7942. Funct Plant Biol 29: 131–149

Price GD, Badger MR, Woodger FJ, Long BM (2008) Advances in understanding the cyanobacterial CO_2-concentrating-mechanism (CCM): functional components, C_i transporters, diversity, genetic regulation and prospects for engineering into plants. J Exp Bot 59: 1441–1461

Raupach MR, Marland G, Ciais P, Le Quere C, Canadell JG, Klepper G, Field CB (2007) Global and regional drivers of accelerating CO_2 emissions. Proc Natl Acad Sci USA 104: 10288–10293

Raven JA, Falkowski PG (1999) Oceanic sinks for atmospheric CO_2. Plant Cell Environ 22: 741–755

Riebesell U, Tortell PD (2011) Effects of ocean acidification on pelagic organisms and ecosystems. In: Gattuso J-P, Hansson L (eds) Ocean Acidification. Oxford University Press, Oxford, pp 99–121

Rokitta SD, Rost B (2012) Effects of CO_2 and their modulation by light in the life-cycle stages of the coccolithophore *Emiliania huxleyi*. Limnol Oceanogr 57: 607–618

Rost B, Kranz SA, Richter KU, Tortell PD (2007) Isotope disequilibrium and mass spectrometric studies of inorganic carbon acquisition by phytoplankton. Limnol Oceanogr Methods 5: 328–337

Rost B, Zondervan I, Wolf-Gladrow D (2008) Sensitivity of phytoplankton to future changes in ocean carbonate chemistry: current knowledge, contradictions and research directions. Mar Ecol Prog Ser 373: 227–237

Sandh G, El-Shehawy R, Diez B, Bergman B (2009) Temporal separation of cell division and diazotrophy in the marine diazotrophic cyanobacterium *Trichodesmium erythraeum* IMS101. FEMS Microbiol Lett 295: 281–288

Sandh G, Ran LA, Xu LH, Sundqvist G, Bulone V, Bergman B (2011) Comparative proteomic profiles of the marine cyanobacterium *Trichodesmium erythraeum* IMS101 under different nitrogen regimes. Proteomics 11: 406–419

Shi DL, Kranz SA, Kim JM, Morel FMM (2012) Ocean acidification slows nitrogen fixation and growth in the dominant diazotroph *Trichodesmium* under low-iron conditions. Proc Natl Acad Sci USA 109: E3094–E3100

Sterner RW, Elser JJ (2002) Ecological Stoichiometry: The Biology of Elements from Molecules to the Biosphere. Princeton University Press, Princeton

Wang QF, Li H, Post AF (2000) Nitrate assimilation genes of the marine diazotrophic, filamentous cyanobacterium *Trichodesmium* sp. strain WH9601. J Bacteriol 182: 1764–1767

Wolf-Gladrow DA, Zeebe RE, Klaas C, Koertzinger A, Dickson AG (2007) Total alkalinity: The explicit conservative expression and its application to biogeochemical processes. Mar Chem 106: 287–300

Zehr JP, Braun S, Chen YB, Mellon M (1996) Nitrogen fixation in the marine environment: Relating genetic potential to nitrogenase activity. J Exp Mar Biol Ecol 203: 61–73

Edited by D. Campbell